Research Square

Preprints are preliminary reports that have not undergone peer review.
They should not be considered conclusive, used to inform clinical practice,
or referenced by the media as validated information.

Adsorption of trans-cinnamamide on pristine and functionalized fullerene: A DFT study

Nubia Saavedra Cruz
Benemérita Universidad Autónoma de Puebla
Alejandro Bautista Hernández
Benemérita Universidad Autónoma de Puebla
Martín Salazar Villanueva
martin.salazar@correo.buap.mx

Benemérita Universidad Autónoma de Puebla
Avelino Cortes Santiago
Benemérita Universidad Autónoma de Puebla
Mauricio Pacio Castillo
Benemérita Universidad Autónoma de Puebla
Wilfredo Ibarra Hernández
Benemérita Universidad Autónoma de Puebla
Odilón Vázquez Cuchillo
Instituto Tecnológico de Puebla
Marco Antonio Meraz Melo
Instituto Tecnológico de Puebla
Carlos Tepech Carrillo
Instituto Tecnológico de Puebla

Research Article

Keywords:

Posted Date: November 13th, 2026

DOI: https://doi.org/10.21203/rs.3.rs-11485596/v1

License: This work is licensed under a Creative Commons Attribution 4.0 International License.
Read Full License

Additional Declarations: No competing interests reported.

Adsorption of trans-cinnamamide on pristine and functionalized fullerene: A DFT study

N. Saavedra Cruz[1,2], A. Bautista Hernández[2], M. Salazar Villanueva[2]*, A. Cortes Santiago[1], M. Pacio Castillo[1], W. Ibarra Hernández[2], O. Vázquez Cuchillo[3], M. A. Meraz Melo[3], and C. Tepech Carrillo[1,3]*

[1]*Centro De Investigación En Dispositivos Semiconductores, Del Instituto De Ciencias De La Universidad Autónoma De Puebla, Av. 14 Sur Col Jardines De San Manuel, Ciudad Universitaria, Puebla, Pue., México.*

[2]*Benemérita Universidad Autónoma de Puebla, Facultad de Ingeniería, Apdo. Postal J-39, Puebla, Pue., 72570, México.*

3 Depto. Metal-Mecánica, Tecnológico Nacional de México I. T. Puebla, Av. Tecnológico 420, Col. Maravillas, Puebla, 72220, Puebla, México.

Corresponding authors:

carlos.tepech@correo.buap.mx

martin.salazar@correo.buap.mx

Abstract

Density functional theory (DFT) calculations were performed to determine adsorption energies (Eads), frontier molecular orbitals (HOMO and LUMO), charge transfer (Q), and partial density of states (PDOS) for the interaction of trans-cinnamamide (CM) with pristine C_{60} and TiO_2-functionalized C_{60} (C_{60}-TiO_2). For pristine C_{60}, these quantum-chemical parameters indicate weak adsorption or desorption, depending on the configuration. By contrast, functionalization markedly increases the magnitude of Eads relative to pristine C_{60} because bonds form between the Ti atom of C_{60}-TiO_2 and C or N atoms of CM in the two most favorable configurations. Charge transfer from the functionalized fullerene to CM

further enhances adsorption. The energy-gap (Eg) values indicate that semiconductor-like electronic behavior is retained after adsorption for all systems analyzed. The contribution of "d" electrons is associated with the enhanced adsorption. Solvated Eads values are lower in magnitude than those obtained in the gas phase; nevertheless, the interaction remains sufficiently strong for potential sensing or storage applications. Overall, TiO_2-functionalized C_{60} appears to be a promising system for capturing CM in both the gas and aqueous phases.

1. Introduction

The development of molecular and nanostructured materials capable of establishing specific interactions with organic molecules has attracted considerable interest because of their potential applications in photocatalysis, sensing, molecular transport, and optoelectronic systems [1-6]. In this context, C_{60} fullerene is a promising candidate because its surface can interact with organic molecules through noncovalent interactions, including dispersion and pi-related interactions, whose strength and character depend on the chemical nature and spatial arrangement of the interacting species [7, 8]. Theoretical investigations of C_{60} complexes with aromatic hydrocarbons have shown that dispersion contributions play a major role in stabilizing these supramolecular assemblies [7], whereas experimental and theoretical studies involving C_{60} and halogenated aromatic molecules have likewise demonstrated that pi-pi stacking, halogen bonding, and F-pi interactions can contribute to the formation of stable supramolecular complexes [8]. These findings establish C_{60} fullerene as a suitable molecular platform for investigating the structural and energetic factors that govern adsorption and noncovalent molecular recognition. The adsorption properties of C_{60} can be further modified through chemical functionalization or interaction with inorganic

components. DFT studies have shown that incorporating transition metals into C_{60} can substantially alter its interaction with small molecules, leading to changes in adsorption strength and electronic structure [9]. Similarly, theoretical investigations of metal oxide adsorption on C_{60} have demonstrated that fullerene-metal oxide complexes can modify the electronic properties of the fullerene and create new chemical sites for molecular adsorption [10]. The interaction of pristine fullerene with extended surfaces also depends strongly on the nature of the substrate and the geometry of the interface, emphasizing the importance of structural configuration in determining the electronic and adsorption properties of fullerene-based systems [11]. It should also be noted that DFT studies of fullerene derivatives indicate that calculated electronic properties, including HOMO and LUMO energies and the corresponding energy gaps, can be sensitive to the choice of exchange-correlation functional [12]. In addition, DFT studies have demonstrated that heteroatom doping can substantially modify the electronic structure and chemical reactivity of C_{60}, thereby enhancing its affinity for pharmaceutical molecules. For example, Nattagh et al. [13] investigated aspirin adsorption on pristine C_{60} and B- and N-doped fullerenes. Their results indicated that aspirin interacts relatively weakly with pristine C_{60}, whereas incorporation of B and N significantly modifies the adsorption behavior through predominantly electrostatic effects. Fekri et al. investigated metronidazole adsorption on pristine and Si-, B-, and Al-doped C60 using DFT calculations at the B3LYP/6-31G(d,p) level. The doped systems exhibited favorable adsorption and stabilization energies, together with changes in frontier-orbital characteristics and thermodynamic descriptors. These findings indicate that heteroatom incorporation can be used to tune the electronic reactivity and drug-binding capability of fullerene-based nanocarriers [14]. Similar behavior was reported by Apriati et al., who investigated the adsorption of paracetamol and hydroxyurea on pristine and Si-doped C_{60} using DFT. The

observed changes in charge distribution further demonstrated that electronic redistribution between the drug and the modified fullerene plays an important role in stabilizing the adsorbed complexes [15]. Another approach to enhancing the drug-loading capability of C_{60} involves the incorporation of metallic species. Esrafili and Khan investigated the adsorption of 5-fluorouracil (5FU) on alkali-metal-decorated C_{60} using first-principles calculations. Their results demonstrated that metal decoration can substantially enhance the interaction between C_{60} and the anticancer drug, whereas solvent effects reduce the magnitude of the adsorption energies, emphasizing the need to consider the surrounding environment when assessing fullerene-based nanocarriers for biomedical applications [16]. Emamjome Koohbanani et al. [17] and Mahdi et al. [18] showed how surface functionalization can modify the electronic and structural characteristics of fullerene-based carriers, while molecular dynamics simulations provide complementary information on the stability of drug-nanocarrier complexes in aqueous environments. Cinnamamide derivatives have also attracted attention because of their structural versatility and characteristic intermolecular interactions. In particular, trans-cinnamamide (CM) contains a conjugated alpha,beta-unsaturated amide moiety linked to an aromatic ring, providing a molecular framework capable of participating in hydrogen bonding and other noncovalent interactions. Crystallographic studies have demonstrated that trans-cinnamamide can adopt well-defined molecular arrangements in the solid state and undergo structural transformations associated with photodimerization [19, 20]. Studies of substituted cinnamamide derivatives have further shown that changes in molecular substituents can modify conformational characteristics and intermolecular hydrogen-bonding patterns [21, 22]. Collectively, these studies demonstrate that drug-fullerene interactions are strongly influenced by the chemical composition and electronic structure of the nanocarrier. Incorporation of a TiO_2 cluster can introduce new

structural and electronic features at the carbon-oxide interface, potentially modifying charge transfer and interactions with drug molecules. This study therefore systematically compares adsorption energies (Eads), charge transfer (Q), interaction distances (Dx), and HOMO-LUMO characteristics to determine whether incorporation of TiO2 promotes CM adsorption relative to pristine fullerene.

2. Computational details

Pristine (C_{60}) and functionalized (C_{60}-TiO_2) fullerenes were used as substrates, and the CM molecule was initially positioned in parallel and perpendicular orientations relative to the substrates. Full DFT calculations were then performed to determine the physicochemical properties of the systems. Geometry optimizations for all systems were carried out with the DMol3 program [23] using DFT [24] and the following computational settings. The M06-L functional [25] was selected because it provides an appropriate description of noncovalent interactions relevant to the adsorption process. All-electron calculations were performed using a double-numerical basis set with polarization functions (DNP), which is comparable in quality to 6-31G(d,p). A Fermi smearing of 0.005 Ha was employed. To accelerate SCF convergence, direct inversion in the iterative subspace (DIIS) was used with a maximum subspace size of 6. The convergence thresholds for the energy gradient and atomic displacement were set to 1 x 10^-5 eV A^-1 and 5 x 10^-4 A, respectively. The charge-density and total-energy convergence criteria were 1 x 10^-6 and 1 x 10^-5 eV, respectively. A global orbital cutoff of 4.4 A was used to construct the numerical basis sets. No spin constraints were imposed. The optimized systems exhibited a multiplicity of M = 1 and no magnetic moment. During the spin-unpolarized self-consistent calculations, the density and energy

tolerances were set to 10^-6 e/bohr^3 and 10^-6 hartree, respectively. For the lowest-energy structures, the energy gaps (Eg) were calculated as the difference between the LUMO and HOMO energies. The adsorption energies (Eads) were calculated using the following expressions:

$$E_{ads} = E\,(C_{60}–CM) – [E\,(C_{60}) + E\,(CM)$$

$$E_{ads} = E\,(C_{60}–TiO_2–CM) – [E\,(C_{60}–TiO_2) + E\,(CM)]$$

where E (C_{60}–TiO_2–CM), E (C_{60}–CM), E (C_{60}–TiO_2), E (C_{60}), and E(CM) are the total energies of the functionalized fullerene-CM complex, pristine fullerene-CM complex, functionalized fullerene, pristine fullerene, and isolated CM molecule, respectively. The basis-set superposition error (BSSE) correction was not applied to the Eads values because DMol3 employs nearly complete numerical basis sets for the separated atoms [26]. Hirshfeld population analysis was used to monitor charge transfer between the substrates and the CM molecule [27]. In addition, energy calculations and geometry optimizations including solvent effects were performed using the conductor-like screening model (COSMO) as a first approximation for simulating biological and wastewater environments [28, 29]. Adsorption in water was investigated using a dielectric constant of 78.4 to approximate biological fluids.

3. Results and discussion

3.1 Adsorption of trans-cinnamamide on pristine C_{60}

The analysis of different orientations of trans-cinnamamide (CM) on pristine fullerene (C_{60}) makes it possible to evaluate how the spatial arrangement of the adsorbate relative to the local topology of C_{60} influences complex stability. For this purpose, 11 configurations were considered. The nonpolar region of the molecule, corresponding to the aromatic ring, the

polar region associated with the amide group, and the intermediate region of trans-cinnamamide were positioned over the center of a hexagonal ring, a pentagonal ring, or a bond shared by five- and six-membered rings of C_{60} (Figure 1). These structural configurations were considered to distinguish the effects of molecular orientation and the chemical nature of each adsorbate region, including variations in contact area, intermolecular distance, and possible π–π dispersive and electrostatic interactions. This strategy enables identification of the most stable adsorption structures without assuming a priori a preferred site on the fullerene surface. As shown in Table 1, the E_{ads} values reveal that adsorption depends on both the molecular region of CM involved and the local topology of the C_{60} surface. For the nonpolar region of CM, the E_{ads} values at the pentagonal, hexagonal, and five-six bond adsorption sites are -0.0360, -0.0161, and -0.0482 eV, respectively. The maximum difference in E_{ads} is approximately 0.0321 eV, indicating weak adsorption. Similar behavior is observed for the intermediate region, with adsorption energies of -0.0785, -0.0913, and -0.0872 eV at the pentagonal, hexagonal, and five-six bond sites, respectively. The maximum difference in E_{ads} is 0.0128 eV, confirming that the local topology of C_{60} has only a limited energetic influence for this molecular region. Unlike the other regions analyzed, the polar region exhibits the weakest adsorption. The configurations at the pentagonal and hexagonal sites have very similar E_{ads} values of -0.0023 and -0.0052 eV, respectively, whereas the configuration at the five-six bond site exhibits an unfavorable positive adsorption energy. Overall, the favorable adsorption-energy values for the three adsorption sites are close to one another, ranging from approximately -0.0913 to -0.0023 eV, which indicates weak adsorption. In addition, differences in E_{ads} among these configurations

are smaller than 0.05 eV; therefore, no significant preference for a specific region of the C60 surface is evident.

System	E_{ads}	HOMO	LUMO	Eg	D_{c-x}	Q(c)	Q(x)
C_{60}–CM–1	-0.036	5.626	3.831	1.795	3.304	0.009	0.0100
C_{60}–CM–2	-0.002	5.592	3.829	1.762	3.132	0.009	-0.0540
C_{60}–CM–3	-0.079	5.597	3.846	1.750	3.192	0.011	0.0100
C_{60}–CM–4	-0.005	5.634	3.863	1.771	3.299	0.011	-0.0540
C_{60}–CM–5	-0.016	5.596	3.807	1.789	3.274	0.011	-0.0090
C_{60}–CM–6	-0.091	5.571	3.848	1.723	3.163	0.013	0.0090
C_{60}–CM–7	0.928	5.051	4.178	0.872	1.568	0.029	-0.014
C_{60}–CM–8	-0.054	5.638	3.876	1.762	3.202	0.010	-0.009
C_{60}–CM–9	-0.043	5.640	3.899	1.741	3.244	0.012	0.010
C_{60}–CM–10	0.155	5.589	3.788	1.801	0.565	0.001	0.098
C_{60}–CM–11	0.174	5.756	3.945	1.811	2.846	0.009	0.026

Table 1. Adsorption energies (E_{ads}), HOMO and LUMO orbital energies, gap energies are in eV. Distance from carbon atom (c) of C_{60} toward the closest atom of CM (x) (D_{c-x}) in Å, whereas electronic charge of carbon atom (C_{60}) and carbon or hydrogen atom of CM molecule, both parameters at adsorption site in **e**. All of them are in gas phase.

Furthermore, within each molecular region, configurations in which the intermediate region of CM is oriented toward the surface exhibit the most stabilizing interactions within their respective groups. These results suggest that local topological variations on the C_{60} surface have a relatively minor influence on the stability of the most favorable configurations, whereas the orientation of the adsorbed molecule may play a more important role. Thus, distance values from atom of carbon (C_{60}) to closest atom of CM molecule at adsorption site (D_{c-x}) are larger than 3 Å, excepting for C_{60}–CM–7, C_{60}–CM–10, and C_{60}–CM–11 respectively. These larger values are associated with low E_{ads} values; nevertheless, the systems with values shorter than 3 Å are associated with desorption process; hence, these distances lead to instability to system.

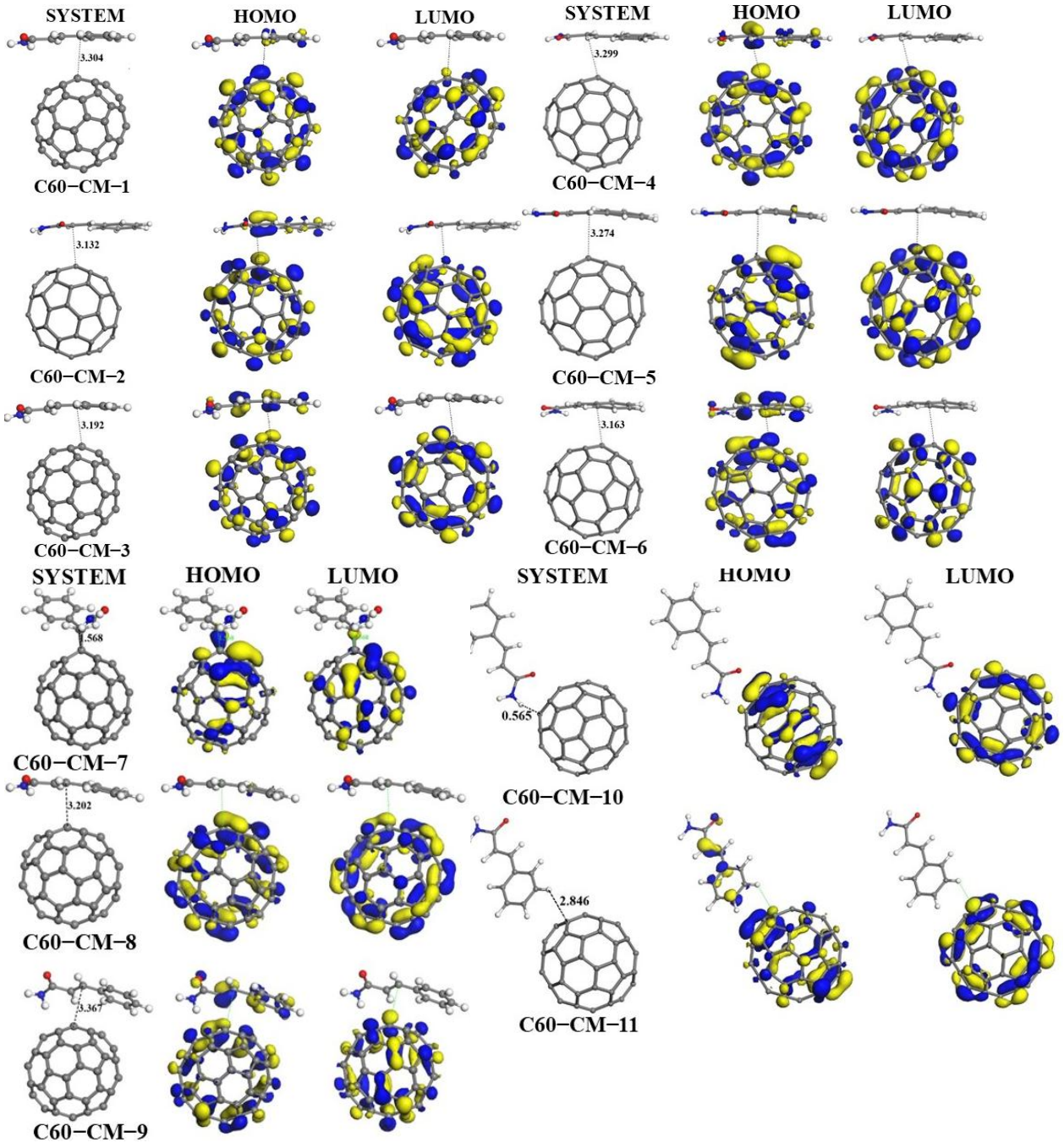


Figure 1. The HOMO and LUMO iso-surfaces of C_{60}–CM systems are depicted. Red, blue, white and gray ball mean oxygen, nitrogen, hydrogen and carbon atoms, respectively. Distances between substrate and CM are in Å. The iso-surfaces are plotted at 0.03 eV/Å^3.

The distances from a carbon atom of C_{60} to the nearest atom of CM at the adsorption site (Dc-x) are generally greater than 3 A. These relatively large separations are consistent with

weak interactions in the favorable adsorption configurations [30]. The calculated charge-transfer values are small, indicating limited electronic redistribution between C_{60} and CM. Furthermore, these results suggest that pristine C_{60} is not an effective substrate for strongly binding CM. Analysis of the frontier molecular orbitals provides complementary information on the adsorption process. For the pristine C_{60}-CM systems, Eg ranges from 0.872 to 1.811 eV. Most adsorbing configurations exhibit Eg values close to 1.7 eV, whereas the C_{60}-CM-7 configuration has the smallest Eg and an unfavorable positive adsorption energy. As shown in Figure 1S (Supporting Information), the HOMO and LUMO energies of the C_{60}-CM systems change only slightly relative to pristine fullerene, consistent with the weak adsorption observed for these complexes. Thus, HOMO and LUMO iso-surfaces show that the frontier-orbital density is concentrated mainly on the fullerene, with only a small or negligible contribution on CM, particularly for configurations with unfavorable adsorption energies. The LUMO is likewise localized predominantly on the fullerene, including the adsorption region. This frontier-orbital distribution is consistent with the weak interaction between pristine C_{60} and CM. The PDOS plots provide complementary evidence: “s” and “p” states contribute to the HOMO, whereas the LUMO is dominated by “p” states, as shown in Figure 2S of the Supporting Information. After full geometry optimization with the solvation model, the E_{ads} values and electronic properties change only modestly relative to the gas-phase results. Thus, adsorption of CM on pristine C_{60} remains weak in both environments. To improve the adsorption capacity, C_{60} was functionalized with a TiO_2 cluster, as discussed in the following section.

3.2 Adsorption of CM on C_{60}-TiO_2

For each system, the initial CM configurations were placed around the TiO_2 cluster and then fully optimized. The resulting adsorption energies, intermolecular distances, and frontier molecular-orbital energies were used to characterize the interaction between CM and the functionalized fullerene. Table 2 shows that incorporation of the TiO_2 cluster enhances adsorption relative to pristine C_{60}. At the M06-L level, the C_{60}–TiO_2–CM complexes exhibit adsorption energies from -1.440 to -0.269 eV, except for C_{60}–TiO_2–CM–3, which has an unfavorable positive E_{ads} value of 0.722 eV. Among the favorable configurations, C60–TiO_2–CM–2 has the most negative adsorption energy, followed by C_{60}–TiO_2–CM–1 and C_{60}–TiO_2–CM–4. This tendency is consistent with the interaction distances and charge-transfer values in Table 2. The shortest adsorption-site distances ($D_{F\text{-}CM}$) are associated with the most favorable E_{ads} values. Moreover, these distances are shorter than those found for pristine C_{60}. Charge transfer in the strongly adsorbed configurations occurs mainly from the Ti-containing functionalized fullerene toward CM. In C_{60}–TiO_2–CM–1 and C_{60}–TiO_2–CM–2, the interaction involves Ti and a C or N atom of CM and is associated with favorable adsorption. By contrast, configurations involving an O atom of the functionalized fullerene and an H atom of CM show weaker or unfavorable adsorption. C_{60}–TiO_2–CM–2 exhibits the strongest adsorption and the largest calculated charge redistribution among the configurations considered.

The Eg values range from 1.155 up to 1.441 eV, these are smaller than pristine cases; however, they are associated with better E_{ads} values. On the other hand, the HOMO and LUMO values of the four C_{60}–TiO_2–CM systems have a pronounced shift respect to substrate (C_{60}–TiO_2), this effect is associated to good adsorption, unlike to observed for pristine case

(see Figure 1S, supporting information). Thus, the higher values of HOMO and LUMO than substrate are related to desorption process.

System	E_{ads}	HOMO	LUMO	Eg	Q(x)	Q(CM)	$D_{F\text{-}CM}$
C_{60}–TiO_2–CM–1	-1.213	5.254	4.098	1.155	0.511	-0.012	2.511
C_{60}–TiO_2–CM–2	-1.440	5.273	3.994	1.278	0.601	-0.126	2.240
C_{60}–TiO_2–CM–3	0.722	5.641	4.200	1.441	-0.268	0.115	2.799
C_{60}–TiO_2–CM–4	-0.269	5.505	4.109	1.396	-0.375	0.042	2.698
C_{60}–TiO_2–CM–1(w)	-0.709	5.313	3.931	1.382	0.524	-0.001	2.49
C_{60}–TiO_2–CM–2(w)	-0.924	5.337	3.896	1.440	0.651	-0.138	2.219
C_{60}–TiO_2–CM–3(w)	-0.088	5.371	3.910	1.461	-0.284	0.138	2.863
C_{60}–TiO_2–CM–4(w)	0.022	5.342	3.905	1.438	-0.391	0.042	2.630

Table 2. Adsorption energies (E_{ads}), HOMO and LUMO orbital energies, gap energies (Eg) are in eV. Electronic charge of titanium or oxygen atom of C_{60}–TiO_2 system Q(x) and the closest atom of CM molecule Q(CM) in **e**, whereas, distance from titanium or oxygen atom of C_{60}–TiO_2 system toward the closest atom of CM in Å ($D_{F–CM}$), distances between substrate and CM molecule are in Å.

In this sense, the iso-surfaces frontier molecular orbitals provide complementary information regarding the electronic response of the complexes due to adsorption process can modify the electronic structure of the functionalized nano-system. From Figure 2, HOMO iso-surface is located around Fullerene for the four cases; nevertheless, at adsorption site is shown an electronic contribution of $d_{x^2-y^2}$ orbital on titanium atom for C_{60}–TiO_2–CM–1 and C_{60}–TiO_2–CM–2 cases, unlike for C_{60}–TiO_2–CM–3 and C_{60}–TiO_2–CM–4 cases, this iso-surfaces is concentrated on oxygen atom with π–π^* stacking. For LUMO, this iso-surface is distributed for the same two cases later, for the first one this is located on CM molecule and TiO_2 cluster, at adsorption site; hence, this zone is chemically active. Unlike the above, the second case this electronic distribution is located just on C_{60}–TiO_2 complex, due to CM molecule is not

interacting chemically with CM molecule and the distance is so large to establish good adsorption. The above information is corroborated with PDOS plots, they are depicted in Figure 3. These reveal major contribution of "p" followed for "s" states; however, despite the presence of just one titanium electron, "d" states exhibit considerable contribution due to for large adsorption, this is present at adsorption site and for weak and desorption process, this atom is bonded to one carbon atom of fullerene, this fact is agree with HOMO and LUMO iso-surfaces and their values already commented.

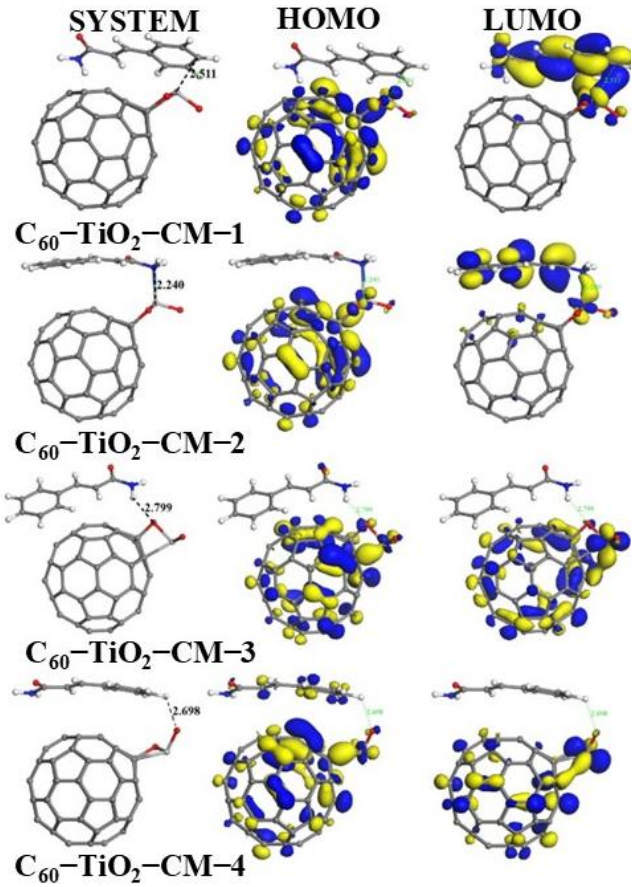


Figure 2. The HOMO and LUMO iso-surfaces of C_{60}–CM–TiO_2 systems are depicted. Red, blue, white and gray ball mean oxygen, nitrogen, hydrogen and carbon atoms, respectively. The iso-surfaces are plotted at 0.03 eV/Å^3.

On the other hand, Calculations including solvation show that the two most strongly adsorbed configurations remain favorable, whereas C_{60}–TiO_2–CM–3 becomes weakly adsorbed and C_{60}–TiO_2–CM–4 becomes unfavorable in the aqueous model. The Eg values, adsorption-site distances, and charge-transfer behavior remain broadly comparable to those obtained in the gas phase. These results indicate that the aqueous environment modifies the adsorption behavior of the less favorable configurations. Overall, the calculated quantum-chemical descriptors suggest that TiO_2-functionalized C_{60} has greater affinity for CM than pristine C_{60} in both gas-phase and aqueous calculations.

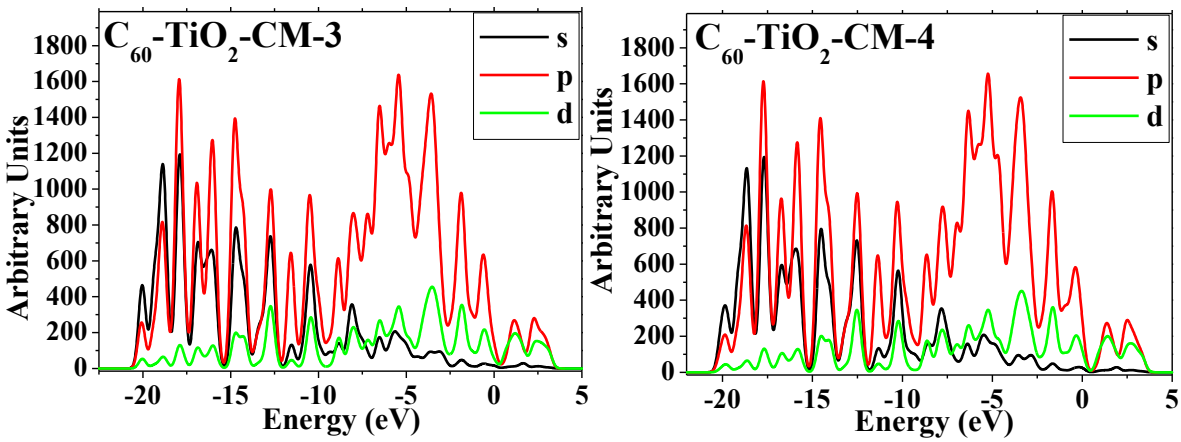


Figure 3. The PDOS plots for C_{60}–TiO_2–CM systems are depicted.

Adsorption energies were also calculated at the PBE/Grimme level to compare the effect of two different theoretical approaches on adsorption by pristine and functionalized fullerenes, using the same SCF conditions described in Section 2. Figure 4 shows that the two approaches yield similar overall adsorption trends, although differences occur for specific configurations, notably C_{60}–TiO_2–CM–3 in the gas phase and C_{60}–TiO_2–CM–4 in water. These differences highlight the sensitivity of predicted adsorption behavior to the chosen

exchange-correlation treatment and support the use of cross-method comparisons when assessing the robustness of the results.

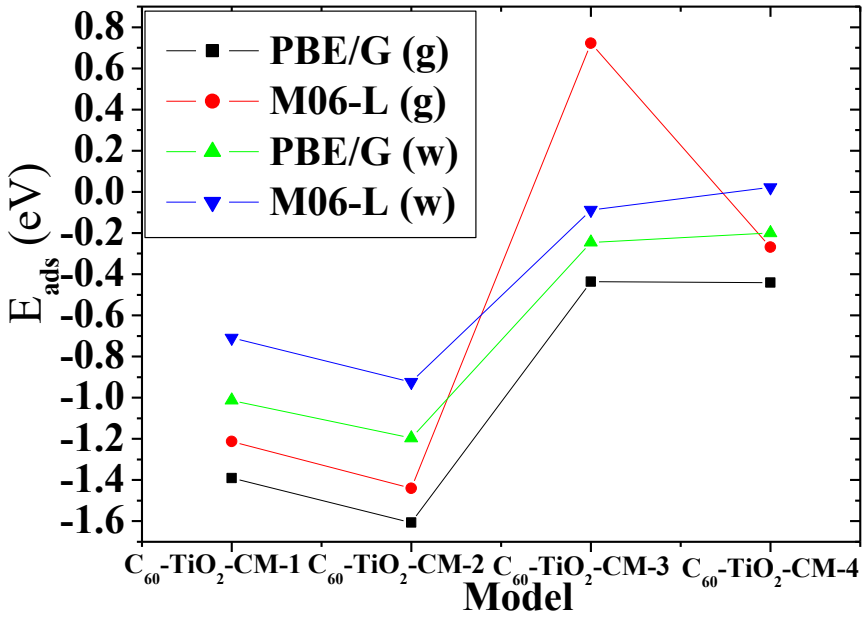


Figure 4. E_{ads} values for functionalized fullerenes at PBE/Grimme and M06-L theory levels in gas (g) and aqueous (w) phase are depicted.

4. Conclusions

DFT calculations were performed to evaluate adsorption process of pristine and functionalized fullerene with CM molecule. Thus, for the pristine C_{60}–CM complexes, it is revealed a pronounced dependence of the adsorption energy on the molecular orientation of CM relative to the fullerene surface. Parallel and perpendicular orientations are associated with weak adsorption and desorption, respectively. For pristine fullerene, E_{ads} values range from -0.091 up to 0.928 eV: hence, it is elucidated adsorption and desorption process are led by weak chemical interactions associated with Van der Waals forces, this effect is proper to systems based on carbon atoms. In aqueous phase these E_{ads} values decrease respect to gas phase. Therefore, pristine fullerene is not candidate to chemically interact with CM molecule

either gas or aqueous phase. On the other hand, TiO_2 functionalization emerges as an important factor governing the adsorption and electronic structure of pristine system, this hybrid system (C_{60}–TiO_2) exhibited enhances adsorption capacity respect to pristine one based on E_{ads} values. These nominal values fall in the range -0.269 ≤E_{ads} ≤-1.440 eV and for desorption, a value of 0.772 eV is exhibited, respectively. The electronic transference from titanium atom (C_{60}–TiO_2) toward carbon and nitrogen atom (CM) is favorable to adsorption, unlike reverse process from hydrogen atoms (CM) toward oxygen atom (C_{60}–TiO_2), this generates weak interaction and desorption, respectively. Nevertheless, in aqueous phase these values are reduced compared to gas phase as well as a transition is found, C_{60}–TiO_2–CM–3 system shows weak interaction whereas C_{60}–TiO_2–CM–4 is related to desorption, respectively. From HOMO, LUMO iso-surfaces and PDOS plots is inferred that contribution of "d" states play a principal role in adsorption process. Thereby, this functionalized fullerene emerges as good candidate to sense or storage this CM molecule either gas or aqueous phase respectively.

5. The authors declare that no separate or external funding was received for this work.

6. References

[1] Xu C, Ravi Anusuyadevi P, Aymonier C, Luque R, Marre S (2019) Nanostructured materials for photocatalysis. Chem Soc Rev 48(14):3868–3902. Doi.org/10.1039/C9CS00102F

[2] Wang Z, Li M, Bu H, Zia D S, Dai P, Liu J W (2023) Nanomaterials for molecular recognition: Specific adsorption and regulation of nanozyme activities. Mater. Chem. Front. 7(17):3625–3640. Doi.org/10.1039/D3QM00208J

[3] Ostroverkhova O (2016) Organic optoelectronic materials: Mechanisms and applications. Chem. Rev. 116(22):13279–13412. Doi.org/10.1021/acs.chemrev.6b00127

[4] Dong J, Yan C, Chen Y, Zhou W, Peng Y, Zhang Y, Wang L N, Huang Z H (2022) Organic semiconductor nanostructures: Optoelectronic properties, modification strategies, and

photocatalytic applications. J Mater Sci Technol 113:175–198. Doi.org/10.1016/j.jmst.2021.09.002

[5] Zhang Y, Fang F, Li L, Zhang J (2020) Self-assembled organic nanomaterials for drug delivery, bioimaging, and cancer therapy. ACS Biomater Sci Eng 6:4816–4833. Doi.org/10.1021/acsbiomaterials.0c00883

[6] Steiner A M, Lissel F, Fery A, Lauth J, Scheele M (2021) Prospects of coupled organic–inorganic nanostructures for charge and energy transfer applications. Angew Chem Int Ed 60(3):1152–1175. Doi.org/10.1002/anie.201916402

[7] Zhang Y, Wang W, Wang Y-B (2017) The nature of the noncovalent interactions between fullerene C60 and aromatic hydrocarbons. Comput Theor Chem 1122:34–39. Doi.org/10.1016/j.comptc.2017.11.004

[8] Zhang Y, Wang J-G, Sun X, Liu Q, Wang W, Wang Y-B (2018) Supramolecular interactions of fullerene C60 with 1,3,5-trifluoro-2,4,6-triiodobenzene: a combined theoretical and experimental study. ChemPlusChem 83:470–477. Doi.org/10.1002/cplu.201800174

[9] El Mahdy AM (2016) Density functional investigation of CO and NO adsorption on TM-decorated C60 fullerene. Appl Surf Sci 383:353–366. Doi.org/10.1016/j.apsusc.2016.04.037

[10] Haghgoo S, Nekoei A-R (2021) Metal oxide adsorption on fullerene C60 and its potential for adsorption of pollutant gases; density functional theory studies. RSC Adv 11:17377–17390. Doi.org/10.1039/D1RA02251B

[11] Shi X-Q, Van Hove MA, Zhang R-Q (2012) Survey of structural and electronic properties of C60 on close-packed metal surfaces. J Mater Sci 47:7341–7355. Doi.org/10.1007/s10853-012-6361-y

[12] Rostami Z, Hosseinian A, Monfared A (2018) DFT results against experimental data for electronic properties of C60 and C70 fullerene derivatives. J Mol Graph Model 81:60–67. Doi.org/10.1016/j.jmgm.2018.02.009

[13] Nattagh F, Hosseini S, Esrafili MD (2021) Effects of B and N doping/codoping on the adsorption behavior of C60 fullerene towards aspirin: a DFT investigation. J Mol Liq 342:117459. Doi.org/10.1016/j.molliq.2021.117459

[14] Fekri MH, Bazvand R, Soleymani M, Razavi Mehr M (2020) Adsorption of metronidazole drug on the surface of nano fullerene C60 doped with Si, B and Al: a DFT study. Int J Nano Dimens 11:346–354.

[15] Apriati YN, Kristiawan B, Jannah N, Nugraheni AD, Sholihun (2023) Drug-molecule adsorption onto silicon-doped fullerene: a density functional theory study. Indones J Chem 23:1742–1749. Doi.org/10.22146/ijc.84174

[16] Esrafili MD, Khan AA (2022) Alkali metal decorated C60 fullerenes as promising materials for delivery of the 5-fluorouracil anticancer drug: a DFT approach. RSC Adv 12:3948–3956. Doi.org/10.1039/D1RA09153K

[17] Emamjome Koohbanani SJ, Ahmadi SA, Ghazanfari D, Sheikhhosseini E (2024) Theoretical investigation of fullerene (C60) as nano carrier for anti-cancer drug Axitinib. Carbon Trends 14:100332. Doi.org/10.1016/j.cartre.2024.100332

[18] Mahdi WA, Alhowyan A, Obaidullah AJ (2025) Computational study of carboplatin interaction with PEG-functionalized C60 fullerene as a drug carrier using DFT and molecular dynamics simulations. Sci Rep 15:13707. Doi.org/10.1038/s41598-025-98262-y

[19] Hosomi H, Ito Y, Ohba S (2000) Crystal-to-crystal photodimerization of trans-cinnamamides. Acta Crystallogr B Struct Sci 56:682–689. Doi.org/10.1107/S0108768100002329

[20] Ohba S, Hosomi H, Ito Y (2001) In situ X-ray observation of pedal-like conformational change and dimerization of trans-cinnamamide in cocrystals with phthalic acid. J Am Chem Soc 123:6349–6352. Doi.org/10.1021/ja0034287

[21] Saeed A, Khera RA, Shahid M, Parvez M (2009) N-(4-Nitro-phenyl)cinnamamide. Acta Crystallogr E Struct Rep Online 65:o2078. Doi.org/10.1107/S1600536809030049

[22] Żesławska E, Nitek W, Marona H, Gunia-Krzyżak A (2017) Crystallographic studies of cinnamamide derivatives as a means of searching for anticonvulsant activity. Acta Crystallogr C Struct Chem 73:953–959. Doi.org/10.1107/S2053229617013845

[23] Delley, B. Analytic energy derivatives in the numerical local-density-functional approach. J Chem Phys 1991, 94, 7245–7250. Doi.org/10.1063/1.460208.

[24] Hohenberg, P.; Kohn, W. Inhomogeneous Electron Gas. Phys. Rev. 1964, 136, B864–B871. Doi.org/10.1103/PhysRev.136.B864.

[25] Exploring the limit of accuracy of the global hybrid Meta density functional for main-group thermochemistry, kinetics, and noncovalent interactions, J. Chem. Theor. Comput., 4 (2008), pp. 1849-1868, Doi.org/10.1021/ct800246v

[26] Inada, Y.; Orita, H. Efficiency of numerical basis sets for predicting the binding energies of hydrogen bonded complexes: evidence of small basis set superposition error compared to Gaussian basis sets. J. Comput. Chem. 2008, 29 (2), 225-232. Doi.org/10.1002/jcc.20782.

[27] De Proft, F.; Alsenoy, C. V.; Peeters, A.; Langenaeker, W.; Geerlings, P. Atomic charges, dipole moments, and Fukui functions using the Hirshfeld partitioning of the electron density, J. Comp. Chem. 2002, 23, 1198-1209. Doi.org/10.1002/jcc.10067.

[28] Klamt, A.; Schüürmann, G. "COSMO: A new approach to dielectric screening in solvents with explicit expressions for the screening energy and its gradient", J. Chem. Soc., Perkin Trans. 2, 5, 799-805 (1993).

[29] Andzelm, J.; Kölmel, Ch.; Klamt, A. "Incorporation of solvent effects into the density functional calculations of molecular energies and geometries", J. Chem. Phys., 103, 9312-9320 (1995).

[30] Lorin X Benedict, Nasreen G Chopra, Marvin L Cohen, A Zettl, Steven G Louie, Vincent H Crespi, Microscopic determination of the interlayer binding energy in graphite, Chem. Phys. Lett. 1998, p.p. 490-496. Doi:10.1016/S0009-2614(97)01466-8

Supplementary Files

This is a list of supplementary files associated with this preprint. Click to download.

- SupportinformationTepech.docx